Kidney International, Vol. 54 (1998), pp. 2029–2036

A theoretical four-compartment model to evaluate separate kidney technetium-99m-MAG_3 kinetics in humans

Giovanna Curti, Daniele DeMartini, Bruno Santaniello, Gioconda Taddei, and Giovanni F. Fresco

Nuclear Medicine Service, Department of Internal Medicine, Division of Clinical Methodological Epidemiology, and Department of Endocrinological and Metabolic Sciences, University of Genoa Medical School, Genoa, Italy

A theoretical four-compartment model to evaluate separate kidney technetium-99m-MAG_3 kinetics in humans.

Background. Pharmacokinetic modeling based on compartmentalization has provided a valuable tool to assess the clearance patterns of various glomerular and tubular agents. However, no models have been proposed thus far that combine vascular data and imaging data in order to gain a deeper knowledge on renal pathophysiology, and to obtain more diagnostic information of clinical relevance. To this aim, we propose a four-pool model for the evaluation of separate renal function.

Methods. In a group of ten normal volunteers and twenty patients with various renal diseases, we tested the four-pool model based on the identification of the two kidneys as two distinct pools. This approach made it possible to integrate the separate kidney contributions deriving from *in vivo* imaging data, and allows the researcher to quantitate many parameters specific to each kidney.

Results. The parameters TER_R, TER_L, MRT_R, MRT_L, ν_R, ν_L, $k_{3R\text{-}1}$, $k_{3L\text{-}1}$ permit the normal from abnormal states of renal function to be differentiated, as well as monolateral from bilateral renal disease to be separated within the abnormal function group.

Conclusions. The proposed approach combines the advantages of plasma clearance methods with those derived by gamma-camera imaging, and makes it possible to quantitate the differential renal function. This feature may be clinically relevant in renal transplant donors, where full knowledge of renal pathophysiology could guide the procedure.

In 1955, Sapirstein and coworkers first described a two-compartment approach for the analysis of the plasma clearance curve of (unlabeled) creatinine injected as an i.v. bolus in dogs [1]. Since then, pharmacokinetic modeling based on compartmental analysis has provided a valuable tool to assess the clearance patterns of various glomerular and tubular agents, aimed at gaining both a deeper knowledge of renal pathophysiology and diagnostic information of clinical relevance [2–9].

In particular, Van Stekelenburg et al experimentally tested the application of a two-compartment model for analyzing the radiolabeled hippuran renogram in humans [3], while a six-compartment model, based on gamma-camera renography only, was proposed by Wolf, Buttermann and Pabst [7]. On the other hand, the seven-compartment model proposed by DeGrazia et al, also based on gamma-camera data from multiple areas of interest, included cumulative urinary excretion as well [5]. However, none of these authors made full use of all of the available information, which when dealing with tracer kinetics should also include data on plasma.

In the present study, we propose a four-compartment model whose basic approach takes into account data from both vascular sources (direct blood sampling) and *in vivo* imaging sources (gamma-camera studies). The renal function component is then split into two distinct pools, that is, left kidney and right kidney. Integration of the imaging data with the plasma curve allows the two kidneys to be identified as two distinct pools, as well as in cases of perfectly symmetrical renal function. The proposed four-pool model was tested in different groups of patients in order to define, among the multiple kinetic parameters evaluated, those which provide the most useful information on renal function in normal and in pathological conditions.

METHODS

Study population

Four groups of subjects were studied: (*1*) the control group (N) included 10 healthy volunteers recruited among staff personnel and specialists in training (7 men and 3 women, mean age 42 ± 10 years); (*2*) group P_1 included 6 patients with symmetrical renal damage mostly resulting from chronic glomerulonephritis (5 men and 1 woman, mean age 51 ± 11 years); (*3*) group P_2 included 8 patients with unilateral right damage (6 men and 2 women, mean age 52 ± 8 years); (*4*) group P_3 included 6 patients with unilateral left kidney damage (4 men and 2 women, mean

Key words: kinetic modeling, plasma clearance, diagnostic technique, gamma-camera imaging, transplantation.

Received for publication June 9, 1997
and in revised form June 30, 1998
Accepted for publication July 6, 1998

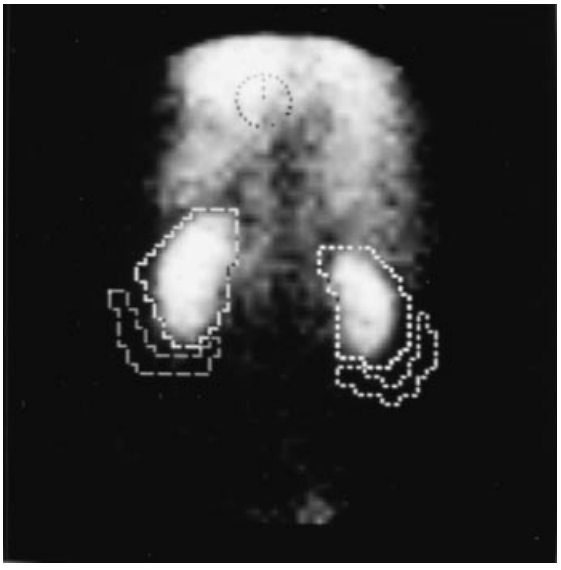

Fig. 1. Gamma-camera display showing the region of interest (ROI) of the heart, kidneys and perirenal regions used as background in a normal subject (case number 6, group N).

age 46 ± 10 years). The twenty patients (group P) altogether were classified on the basis of medical history and the common clinical and laboratory findings including renal time-activity curves of injected ^{99m}Tc-MAG_3. Unilateral damage mostly resulted from the late effect of pyelonephritis due to vesico-ureteral reflux.

Data collection

After adequate hydration, each subject was injected into an antecubital vein with an i.v. bolus of about 37 MBq ^{99m}Tc-MAG_3, supplied as an instant-labeling kit formulation (Technescan MAG_3; Mallinckrodt Medical BV, Petten, Holland), while a vein of the contralateral arm was utilized for blood sampling. For each subject, thirteen 7-ml blood samples were drawn into standard EDTA-anticoagulated vacuum tubes at 5, 10, 20, 30, 45, 60, 75, 90, 105, 120, 150, 180, 210 minutes. A separate standard for ^{99m}Tc-MAG_3 was prepared by dilution in 2000 ml of physiological saline from duplicate syringe. Three-milliliter plasma samples obtained from each blood specimen and 3-ml aliquots of the acqueous standard solution were pipetted into counting tubes and counted using a multichannel Packard Autogamma Spectrometer with a 10% window centered on the 140 keV energy peak of ^{99m}Tc. Before injection, each subject had been positioned supine on the imaging bed of a large-field-of-view gamma camera (Elscint Apex SP6) equipped with a low-energy all-purpose collimator, to acquire posterior views. Dynamic sequences were recorded starting upon tracer injection with a time resolution of 1 frame/3 seconds (64 × 64 pixels) for the first two minutes and of 1 frame/15 seconds for the following 28 minutes. Five regions of interest (ROIs) were selected: the two renal areas, the two perirenal areas, and the cardiac area (Fig. 1). The time-activity curves defined over these five ROIs were normalized by calculating the mean counts per pixel. The counts recorded on renal ROIs were then corrected for: (*1*) background activity in the semilunar ROIs placed around the lower, outer renal margins; (*2*) depth of each kidney, estimated by the formula of Tonnesen et al [10] with a linear attenuation coefficient for ^{99m}Tc radiation in soft tissues equal to 0.153 cm^{-1} [11]; and (*3*) blood pool activity within each kidney. This last correction was performed by determining the blood pool partition coefficient based on the heart and each separate kidney curve, as described previously [12–15]. Using the background-corrected and blood pool-corrected kidney curves, values for the tracer accumulation rates in the right (k_{uR}) and left (k_{uL}) kidneys were then derived (based on the early portion of the activity-time curves). The rates of irreversible loss of radioactivity from the right (k_{oR}) and left (k_{oL}) kidneys were similarly determined, taking into account the early, monoexponential portion of the wash-out phase of the corrected renal activity curves.

Model

The four-pool model consists of the following compartments: (*a*) compartment 1, the fast initial distribution pool, that is, the injection compartment; (*b*) compartment 2, which includes unidentified extravascular and extrarenal spaces; (*c*) compartment 3L, the left kidney; and (*d*) compartment 3R, the right kidney (Fig. 2). Irreversible loss of radioactivity from the system proceeds only from the kidneys to urine.

Data analysis

In each subject, the rates of uptake in the right and left kidneys (k_{uR} and k_{uL}) derived from gamma-camera imaging data were compared with each other. When the difference between k_{uR} and k_{uL} was greater than 20% of their mean value $\overline{k_u}$, that is, when $\Delta\ \% (= | k_{uR} - k_{uL} | / \overline{k_u}) > 20$, the plasma curve determined by *in vitro* counting was fitted to a solution of the system of differential equations of the type: (**Appendix**, Eq. A1)

$$Y(t) = \sum_{i=1}^{4} A_i e^{-\lambda i t} \qquad \text{(Eq. 1)}$$

The 20% threshold was selected on the basis of preliminary evaluations showing that the cumulative error possibly affecting the estimate of k_{uR} and k_{uL}, and consequently their difference, was always lower than 20% of their mean value, even in the least favorable conditions.

In this solution based on four exponentials, Y(t) (KBq/ml/1.73 m^2) indicates plasma concentration at time t (min) normalized to a reference body surface of 1.73 m^2, expressed as % injected dose (ID) (MBq/ml); A_i (% ID/ml/1.73 m^2) is the intercept on the y-axis of the different

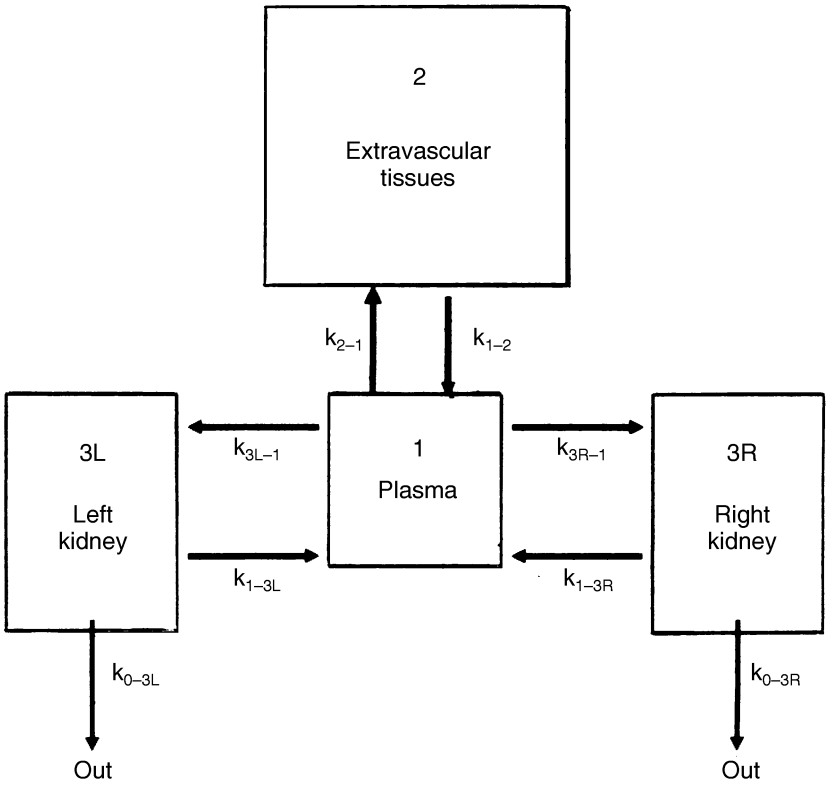

Fig. 2. Schematic representation of the four-compartment model for ^{99m}Tc-MAG_3. The compartment 1 (the injection compartment) is interconnected with the compartment 2 (the extravascular tissues) and with the compartments 3R (the right kidney) and 3L (left kidney). Irreversible loss of radioactivity from the system proceeds only from the kidneys to urine.

components of the plasma curve; and λ_i (min^{-1}) represents the slope of the four components of the curve. In those cases where $\Delta\%$ was ≤ 20, the plasma curve data were fitted to a solution of the type (Appendix, Eq. A2):

$$Y(t) = A_1(1 + t)e^{-\lambda 1t} + \sum_{i=2}^{3} A_i e^{-\lambda it} \qquad \text{(Eq. 2)}$$

This represents a general solution (based on three exponentials) of the characteristic polynomial for the homogeneous linear differential equation when a root λ_1 of multiplicity 2 exists [16–18]; A_1, A_i, λ_1, λ_i have the same meaning as indicated above. This analysis was performed with a commercially available program based on subsequent iterations [19], which also provided an approximation of the variance/covariance matrix of the parameters studied, by minimizing the sum of squares of nonlinear functions [20].

Kinetic parameters

The parameters that characterize the four-pool model include: (*1*) those determined directly from gamma camera studies without assuming any preassigned model structure, and (*2*) those directly quantified by using a combined integral-differential solution [19–22] based on vascular and organ data (heart and kidneys). The first group includes: (*a*) the fractional transfer rates k_{3R-1} and k_{3L-1} (identified as the rates of accumulation in the right anf left kidney, previously indicated as k_{uR} and k_{uL}); (*b*) the fractional transfer rates k_{0-3R} and k_{0-3L} (identified as the corresponding rates of irreversible tracer loss from kidneys to bladder k_{0R} and k_{0L}). The second group of kinetic parameters includes: the volume of the fast initial distribution pool (V_1), the volume of the extravascular pool (V_2), and the volumes of the right and left kidney (V_{3R} and V_{3L}), the fractional transfer rates between compartments k_{1-2}, k_{2-1}, k_{3R-1} and k_{3L-1}. The total tubular excretion rate (TER) and the tubular excretion rate of each kidney, that is, TER_R and TER_L, were also determined (this is a clearance value). In addition, the mean residence time of the tracer in the system, MRT ($MRT = V_{Tot}/TER$), its permanence time in compartments 3R and 3L (MRT_{3R} and MRT_{3L}), that is, the expected interval of time the substance spends in all passages through these compartments, were also estimated. Moreover, t_1, t_2, t_{3R} and t_{3L} were quantified to determine the expected intervals of time the substance spends in each passage through compartments 1, 2, 3R and 3L. Finally, we determined the turnover number, ν_{3R} and ν_{3L}, of compartments 3R and 3L ($\nu_i = MRT_i/t_i$), that is, the expected number of passages of the substance in the same compartments.

Statistical analysis

All data were expressed as mean ± SD. Multivariate Hotelling test was performed considering all variables to compare the group of normal subjects (N, $N = 10$) with that including all patients (P, $N = 20$), and to compare group N

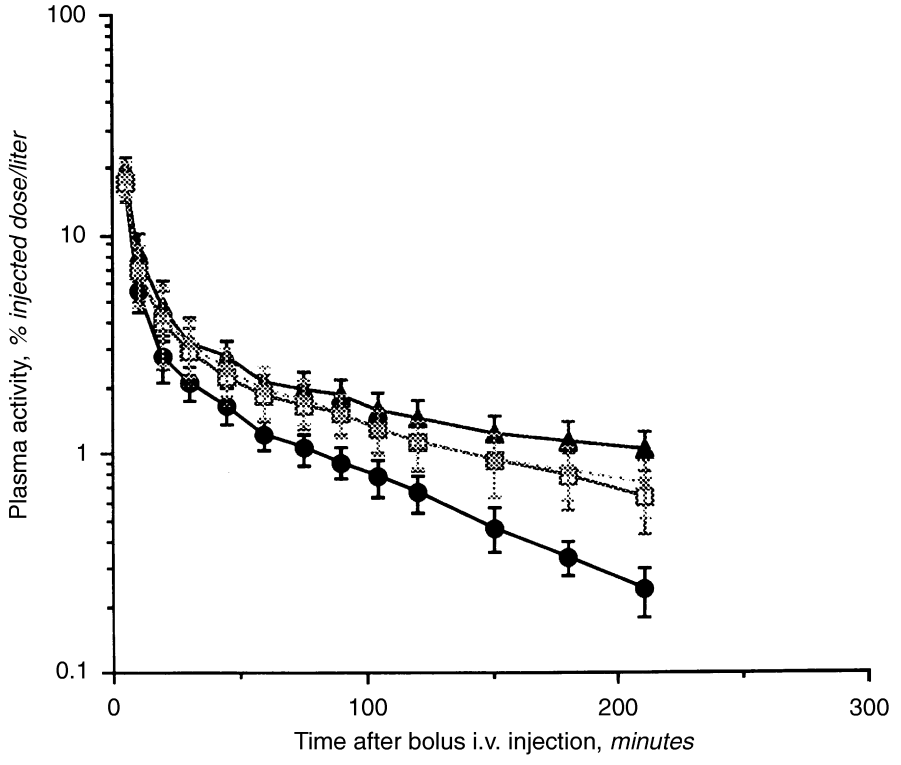

Fig. 3. Mean values and range of the plasma data (expressed as percent of the injected dose per liter) determined in 10 healthy volunteers (group N), in 6 patients with symmetrical renal damage (group P_1), in 8 patients with unilateral right damage (group P_2), and in 6 patients with unilateral left renal damage (group P_3). Symbols are: (●) Group N; (▲) Group P_1; (□) Group P_2; (**X**) Group P_3.

with groups P_1 ($N = 6$), P_2 ($N = 8$), and P_3 ($N = 6$). Univariate analysis of each variable was performed and, in order to compare N with each patient's groups, multiple comparisons using Dunnett's test were performed. All computations were carried out using the SAS 610 program GLM procedure. Probability values lower than 0.05 were considered statistically significant.

RESULTS

Mean values and ranges of the plasma data (expressed as percent of the injected dose per liter), determined in all groups studied are depicted in Figure 3.

Mean values and ranges for the kinetic parameters determined in all groups studied are listed in Table 1. In the six patients with symmetrical renal impairment, the mean value for TER (MAG_3) was significantly lower than in normals (115.8 vs. 306.9 ml/min/1.73 m^2, $P < 0.05$). In these patients we observed increased mean values for V_1 and V_2 compared to the normal values (6.18 vs. 4.48 liter/1.73 m^2, and 12.24 vs. 7.96 liter/1.73 m^2, respectively). The mean residence time (MRT) of the tracer in the system was significantly longer than in normals (192.3 vs. 42.2 min, $P < 0.05$), while the mean number of passages in right and left kidney resulted to be increased with respect to the corresponding normal values (8 vs. 5). In the eight patients with unilateral right renal damage, we observed significantly decreased mean values for $k_{3R\text{-}1}$ and $k_{0\text{-}3R}$ with respect to the normal values ($P < 0.05$), while the $k_{3L\text{-}1}$ and $k_{0\text{-}3L}$ values were not different from the normal values. The opposite was observed in the six patients with unilateral left renal damage where, in presence of normal values for $k_{3R\text{-}1}$ and $k_{0\text{-}3R}$, the $k_{3L\text{-}1}$ and $k_{0\text{-}3L}$ values were markedly decreased. In these patients, we observed increased values for the distribution spaces V_1 and V_2 (8.79 vs. 4.48 liter/1.73 m^2, and 14.06 vs.7.96 liter/1.73 m^2, respectively); the clearance rate in the injured organ was found to be significantly decreased (43.4 vs.151.0 ml/min/1.73 m^2). At the same time, the permanence time in the injured kidney was markedly prolonged (12.9 vs. 4.7 min in group P_2 and 14.2 vs. 5.4 min in group P_3). Nevertheless, in these patients the number of passages required for final exit from the system was the same in both the injured and unaffected kidney, about twofold more than the normal value (10 vs. 5).

Table 2 summarizes the results of multivariate analysis for comparing all groups of our population. In particular, the comparison was carried out between: (*a*) groups N and P; (*b*) between N, P_1, P_2 and P_3; (*c*) and between P_1, P_2 and P_3. Figure 4 depicts fitting of the model-estimated parameters to the experimental plasma clearance curves observed in two representative patients, respectively case number 6 (group N) and case number 19 (group P_3, with unilateral left kidney damage).

DISCUSSION

In this work concerning renal dynamics, we implemented a four compartment model where the deterministic approach allows a derivation of the kinetic parameters that is specific to tissues, with the goals of differentiating normal

Table 1. Mean values and range for the ^{99m}Tc-MAG_3 parameters determined in healthy volunteers (N), in patients with bilateral (P_1), unilateral right (P_2), unilateral left (P_3) renal damage, and in the group (P), which includes all patients with various degree of renal impairment

Parameter	N $N = 10$	P_1 $N = 6$	P_2 $N = 8$	P_3 $N = 6$	P $N = 20$
Model-structure independent parameters					
$k_{3R\text{-}1}$ *min*$^{-1}$	0.064 ± 0.010	0.031 ± 0.009[a]	0.020 ± 0.006[a]	0.065 ± 0.006	0.037 ± 0.021[a]
$k_{3L\text{-}1}$ *min*$^{-1}$	0.061 ± 0.006	0.028 ± 0.008[a]	0.062 ± 0.010	0.021 ± 0.005[a]	0.040 ± 0.021[a]
$k_{0\text{-}3R}$ *min*$^{-1}$	0.21 ± 0.03	0.10 ± 0.02[a]	0.08 ± 0.02[a]	0.20 ± 0.06	0.13 ± 0.06[a]
$k_{0\text{-}3L}$ *min*$^{-1}$	0.20 ± 0.02	0.09 ± 0.04[a]	0.22 ± 0.03	0.09 ± 0.05[a]	0.14 ± 0.07[a]
Four-pool ^{99m}Tc-MAG_3 model parameters					
V_1 *liter/1.73 m*^{2}	4.48 ± 1.08	6.18 ± 1.53[a]	9.00 ± 1.06[a]	8.79 ± 1.12[a]	8.01 ± 1.67[a]
V_2 *liter/1.73 m*^{2}	7.96 ± 1.57	12.24 ± 1.81[a]	14.67 ± 1.08[a]	14.06 ± 1.71[a]	13.79 ± 1.78[a]
V_{3R} *liter/1.73 m*^{2}	0.25 ± 0.02	0.26 ± 0.03	0.24 ± 0.03	0.27 ± 0.02	0.26 ± 0.03
V_{3L} *liter/1.73 m*^{2}	0.26 ± 0.02	0.27 ± 0.03	0.26 ± 0.03	0.24 ± 0.03	0.26 ± 0.03
V_{Tot} *liter/1.73 m*^{2}	12.95 ± 2.46	18.95 ± 3.34[a]	24.17 ± 1.85[a]	23.36 ± 2.62[a]	22.32 ± 3.35[a]
$k_{1\text{-}3R}$ *min*$^{-1}$	0.91 ± 0.21	0.66 ± 0.29	0.64 ± 0.19	1.92 ± 0.31[a]	1.01 ± 0.62
$k_{1\text{-}3L}$ *min*$^{-1}$	0.85 ± 0.23	0.55 ± 0.22	1.95 ± 0.41	0.68 ± 0.20	1.14 ± 0.74
$k_{2\text{-}1}$ *min*$^{-1}$	0.23 ± 0.02	0.29 ± 0.02[a]	0.23 ± 0.02	0.23 ± 0.02	0.25 ± 0.03
$k_{1\text{-}2}$ *min*$^{-1}$	0.13 ± 0.02	0.14 ± 0.01	0.14 ± 0.02	0.14 ± 0.01	0.14 ± 0.01
TER *ml/min/1.73 m*^{2}	306.9 ± 29.7	115.8 ± 46.5[a]	150.4 ± 17.4[a]	152.9 ± 38.2[a]	140.7 ± 36.7[a]
TER_R *ml/min/1.73 m*^{2}	155.9 ± 15.1	58.8 ± 18.0[a]	42.0 ± 11.2[a]	109.5 ± 25.8[a]	68.5 ± 35.9[a]
TER_L *ml/min/1.73 m*^{2}	151.0 ± 20.3	57.0 ± 28.9[a]	108.5 ± 12.0[a]	43.4 ± 16.8[a]	72.3 ± 35.8[a]
MRT *min*	42.2 ± 7.8	192.3 ± 107.4[a]	162.9 ± 25.6[a]	161.5 ± 49.5[a]	171.0 ± 64.3[a]
MRT_{3R} *min*	4.8 ± 0.7	10.9 ± 2.8[a]	12.9 ± 3.7[a]	5.4 ± 1.9	9.8 ± 4.5[a]
MRT_{3L} *min*	5.0 ± 0.6	12.6 ± 4.8[a]	4.7 ± 0.6	14.2 ± 4.8[a]	10.0 ± 5.6[a]
t_1 *min*	2.8 ± 0.2	2.9 ± 0.2	3.2 ± 0.2[a]	3.2 ± 0.3[a]	3.1 ± 0.2[a]
t_2 *min*	7.9 ± 1.2	7.0 ± 0.5	7.1 ± 0.9	7.0 ± 0.4	7.1 ± 0.7[a]
t_{3R} *min*	0.9 ± 0.2	1.5 ± 0.6[a]	1.5 ± 0.4[a]	0.5 ± 0.1	1.2 ± 0.6
t_{3L} *min*	1.0 ± 0.2	1.8 ± 0.8[a]	0.5 ± 0.1[a]	1.4 ± 0.5	1.2 ± 0.7
ν_{3R}	5 ± 1	8 ± 3[a]	9 ± 2[a]	12 ± 4[a]	9 ± 3[a]
ν_{3L}	5 ± 1	8 ± 4	10 ± 3[a]	10 ± 2[a]	9 ± 3[a]

Values are mean ± SD. Comparison were performed using Dunnett's test. [a] $P < 0.05$

from abnormal states of renal function and to achieve deeper knowledge of renal pathophysiology. In previously described models both kidneys were assigned to a single compartment from which any exit of tracer back to plasma was neglected [3, 5–7]. This is not consistent with the true renal dynamics. As a matter of fact, when one considers that in normals about 300 ml of plasma containing ^{99m}Tc-MAG_3 reach the tubular cells every minute [23–25], assigning to kidneys a purely non-active transport function, all tracer should be cleared from plasma in few minutes. Actually, in normals the mean residence time of the substance in the system is about 45 minutes [23, 24], and therefore one should conclude that a significant fraction of tracer per unit time returns from tubular cells to plasma prior to its irreversible exit. Recently Stabin et al adopted a three pool model to assess radiation dosimetry for different renal agents, including ^{99m}Tc-MAG_3 in humans, the structure of which did not exclude the active presence of kidneys as concerns tracer kinetics, similar to our model [9]. The model we propose implies partial removal of the substance at each passage in kidneys, which becomes complete only after various passages through the central plasma compartment. In fact, irreversible losses from the kidney pools are the only routes through which the substance is removed (cleared) from the entire system.

The basic idea of this work is the possibility to fix the structure of the model in a way that is somewhat specific for each single patient and, on the other hand, to modify the type of solution to the system of differential equations (**Appendix**). In order to make this point clear, we subdivided the population studied in two sets. The first set included those subjects in whom a significant difference, not ascribable to errors, existed between the rates of uptake k_{uR} and k_{uL}, consistent with a monolateral renal damage. In this case, the solution is a sum of four exponential terms (**Appendix**, Eq. A1). The other set includes normals and patients with bilateral symmetrical renal damage. In this case the solution is a sum of three exponential terms, together with a linear term that takes into account the presence of a multiple root, caused by a nearly equal rate of equilibration between plasma and two kidneys (**Appendix**, Eq. A2). The latter solution, which allows the compartments 3R and 3L to be "split" (Fig. 2) that otherwise would be "lumped" into a single pool, has been demonstrated mathematically in many standard textbooks and papers [16–18]. The linear term, which is important only at a time earlier than the time at which the function ($t\, e^{-\lambda 1 t}$) reaches the maximum (that is, $t < 1/\lambda_1$), in our cases was always shorter than three minutes. Since the first plasma sample was taken five minutes after i.v. injection of the radiotracer, actually the experimental plasma data were fitted to a sum of three exponential terms, as the contribution of the linear term was negligible. The structure of the model we propose

Table 2. Statistical results derived comparing the kinetic parameters in various groups: N (normal subjects, $N = 10$), P (all patients, $N = 20$), P_1 (patients with bilateral renal damage, $N = 6$), P_2 (patients with unilateral right damage, $N = 8$), and P_3 (patients with unilateral left damage, $N = 6$)

Parameter	N, P ($P = 0.008$) Hotelling test	N, P_1, P_2, P_3 ($P = 0.0039$) Hotelling test	P_1, P_2, P_3[a]
k_{3R-1}	0.0006	0.0001	0.0001
k_{3L-1}	0.0028	0.0001	0.0001
k_{0-3R}	0.0005	0.0001	0.019
k_{0-3L}	0.0064	0.0001	0.013
V_1	0.0001	0.0001	0.009
V_2	0.0001	0.0001	0.0245
V_{3R}	NS	NS	NS
V_{3L}	NS	NS	NS
V_{Tot}	0.0001	0.0001	0.0045
k_{1-3R}	NS	0.0001	0.0001
k_{1-3L}	NS	0.0001	0.0001
k_{2-1}	NS	0.0001	0.0001
k_{1-2}	0.0499	NS	NS
TER	0.0001	0.0001	NS
TER_R	0.0001	0.0001	0.0001
TER_L	0.0001	0.0001	0.0001
MRT	0.0001	0.0001	NS
MRT_{3R}	0.0015	0.0001	0.0002
MRT_{3L}	0.0096	0.0001	0.0003
t_1	0.0069	0.0021	0.0315
t_2	0.0315	NS	NS
t_{3R}	NS	0.0001	0.0004
t_{3L}	NS	0.0001	0.0003
ν_{3R}	0.0003	0.0039	NS
ν_{3L}	0.0007	0.0060	NS

[a] too few degrees of freedom to perform multivariate analysis

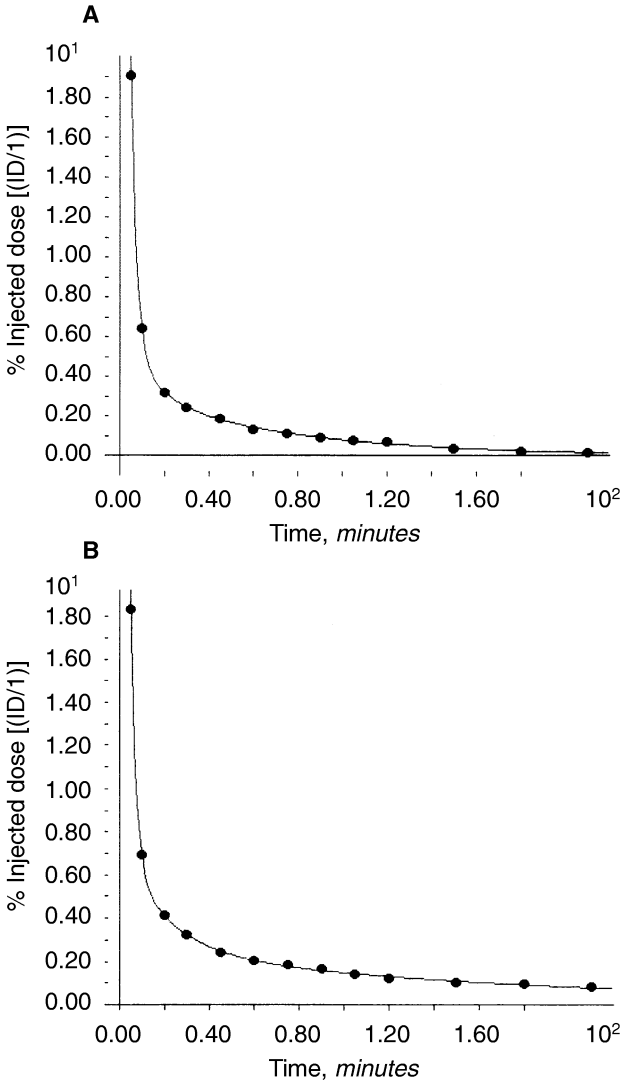

Fig. 4. ^{99m}Tc-MAG_3 plasma data in two cases studied: case number 6 (*A*; group N) and case number 19 (*B*; group P_3, with unilateral left kidney damage). The curve represents the fitting of the model-estimated parameters to plasma data.

implies the acquisition of a number of independent parameters larger than the number of independent differential equations based on the tracer concentration in the four compartments. Thus, in a deterministic approach, plasma data need to be integrated with additional data that we derived from gamma-camera studies. This procedure requires careful evaluation of the factors that allow for a correction of the renal activity curve for background, depth of kidney, and blood activity. The depth of each kidney was determined according to the Tonnesen formula [10], which takes into account weight and height of each subject studied. This approach is correct when the population studied does not include obese individuals and subjects with ectopic kidneys. According to literature [7, 9, 26], we assumed the fractional transfer rates from plasma to kidneys (k_{3R-1} and k_{3L-1}) to be equal to the rates of uptake (k_{uR} and k_{uL}), while the fractional excretion rates (k_{0-3R} and k_{0-3L}) were identified with the rate constants (k_{0R} and k_{0L}) derived from the nephrogram. When considering the mean values and ranges for the pharmacokinetic parameters (Table 1), normal subjects exhibited a mean value of the fast initial distribution volume (V_1) equal to 4.48 liter/1.73 m^2, in good agreement with the theoretical plasma volume.

The volume of compartment 1 was much larger in patients with various renal damage (such as in group P_2, 9.00 liter/1.73 m^2), as was the volume V_2 pertaining to extravascular extrarenal tissues (such as in group P_2, 14.67 liter/1.73 m^2). The values for volumes V_{3R} and V_{3L} were about 0.25 l/1.73 m^2 for both kidneys, slightly greater than the anatomic volume, and this could be the result of an incorrect assumption made about the kidney as a single well-mixed compartment. Statistical analysis indicated the permanence time of the injected tracer in the system (MRT) as a useful parameter for differentiating normal and pathological states. However, this same parameter was unreliable for differentiating various types of renal damage (Table 1), as were the turnover numbers ν_{3R} and ν_{3L} not reliable. On the contrary, parameters k_{1-3R}, k_{1-3L} and k_{2-1} were unreliable in distinguishing normal from pathological

states, but became useful in identifying different types of renal damage.

The mean value for the permanence time of ^{99m}Tc-MAG_3 in kidneys in our population, MRT_{3R} and MRT_{3L}, agrees well with the mean value for the mean parenchymal transit time (MPTT) for ^{99m}Tc-MAG_3 as computed by other authors using the nephrogram deconvolution technique [27]. The values obtained for the fractional transfer rate from each kidney to plasma ($k_{1\text{-}3R}$ and $k_{1\text{-}3L}$) appear to confirm that a great fraction of tracer returns to plasma from kidneys prior to its irreversible loss. This fact is in agreement with the observed mean number of passages of the tracer in each kidney prior to its irreversible removal, which results to be about 5 in normals and about 10 in all patients. The fact that for patients with asymmetrical renal damage the number of passages increases both in the injured kidney and in the unaltered kidney may be explained by a significantly shorter time of each passage in the unaltered kidney (t_{3R} or t_{3L}) with respect to the contralateral injured organ. This observation is consistent with a "vicarious" role of the unaffected kidney related to the impaired function of the contralateral, injured kidney. The total tubular excretion rate (TER) of ^{99m}Tc-MAG_3 we obtained in normal volunteers was equal to 306.9 ± 29.7 ml/min/1.73 m^2, in good agreement with the corresponding values obtained by other authors employing a bicompartmental approach [23–25, 28].

At present, radiotracer plasma clearance methods [4, 23–25, 28–32] provide an accurate determination of total renal function, while they cannot provide a separate study of kidney kinetics. As the present model combines the implicit advantages of plasma clearance methods with those derived by gamma-camera methods [35–37], in spite of its complexity it can be considered a useful tool to achieve deeper knowledge on the pathophysiology of the renal system. The clinical utility of the present approach may arise from the possibility of quantitating the differential renal function (for example, TER_R, TER_L, $k_{3R\text{-}1}$, $k_{3L\text{-}1}$, MRT_R, MRT_L). In patients with unilateral disease, these parameters could guide therapy, particularly if the renal function is severely decreased on one side and a mantained function is on the contralateral side, where nephrectomy may be indicated. However, when disease exists in both kidneys, partial nephrectomy may avoid renal insufficiency. Furthermore, in renal transplant donors it is crucial to quantitate the tubular excretion rate of the remaining kidney. Moreover, the present approach can be used to assess the degree of improved renal function after angioplasty or surgery for renovascular hypertension.

ACKNOWLEDGMENTS

The authors thank Drs. Giuseppe Villa, Elie Catsafados, Fabio Martini and Elham Safaie Semnani for their assistance in the collection of data, and Dr. Giuliano Mariani for helpful discussion in the revision of this manuscript.

Reprint requests to Giovanna Curti, Ph.D., Nuclear Medicine Service, Department of Internal Medicine, University of Genoa Medical School, Viale Benedetto XV, No 6, I-16132 Genoa, Italy.

APPENDIX

In an attempt to define and estimate the kinetic parameters of our four-pool model, we adopted a procedure that combines the sums of exponentials approach with the direct model solution approach [19, 21, 22].

When $\Delta\ \% > 20$, the solution of the system of differential equations is expressed by the equation

$$Yj(t) = \sum_{i=1}^{4} A_{ji} e^{-\lambda i t} \qquad \text{(Eq. A1)}$$

where Yj (t) represents ^{99m}Tc-MAG_3 concentration (% ID/ml/1.73 m^2) in pool j (such as, plasma pool) at time t (min), A_{ji} (% ID/ml/1.73 m^2), and λ_i (min^{-1}) represents the exponential function coefficients and exponents. In the cases where $\Delta\ \% \leq 20$, since a root λ_1 of multiplicity 2 of characteristic polynomial is present, the solution becomes

$$Yj(t) = A_{j1}(1 + t)e^{-\lambda 1 t} + \sum_{i=2}^{3} A_{ji} e^{-\lambda i t} \qquad \text{(Eq. A2)}$$

The direct model solution approach is derived from a set of differential equations based on linear comparmental system.

If $q_i(t)$ represents the quantity of substance in pool i at time t, and $Y(t_r)$ represents the plasma data at time t_r, the following equations are derived directly from the model:

$$dq_1(t)/dt = -(k_{2-1} + k_{3L-1} + k_{3R-1})q_1(t) + k_{1-2}q_2(t) + k_{1-3L}q_{3L}(t) + k_{1-3R}q_{3R}(t) \qquad \text{(Eq. A3)}$$

$$dq_2(t)/dt = +k_{2-1}q_1(t) - k_{1-2}q_2(t) \qquad \text{(Eq. A4)}$$

$$dq_{3L}(t)/dt = +k_{3L-1}q_1(t) - (k_{1-3L} + k_{0-3L})q_{3L}(t) \qquad \text{(Eq. A5)}$$

$$dq_{3R}(t)/dt = +k_{3R-1}q_1(t) - (k_{1-3R} + k_{0-3R})q_{3R}(t) \qquad \text{(Eq. A6)}$$

$$Y\ (t_r) = q_1(t_r)/V_1$$

where V_1 is the initial distribution plasma volume and $r = 1.\ldots.N$ samples of plasma at various times.

The integration of these equations yields the following general solution:

$$q_i(t) = \int_0^t \sum_j k_{ij} q_j(\tau)\, d\tau + q_i(0) = \sum_j k_{ij} \int_0^t q_j(\tau)\, d\tau + q_i(0) \qquad \text{(Eq. A7)}$$

where q_i (t) is expressed as linear combinations of the integral

$$\int_0^t q_j(\tau)\, d\tau$$

If the data are measures of the q_j (t) and are fitted to sum of exponentials on the basis of equation A1, we may write

$$q_j(t) = \sum_{k=1}^{4} A_{jk} e^{-\alpha k t}$$

and substitution into equation A7 yields

$$q_i(t) = \sum_j k_{ij} \sum_{k=1}^{4} A_{jk} \int_0^t e^{-\alpha k \tau}\, d\tau + q_i(0) \qquad \text{(Eq. A8)}$$

or we may write, in the case of equation A2

$$q_j(t) = A_{j1}(1 + t)e^{-\alpha 1t} + \sum_{k=2}^{3} A_{jk}e^{-\alpha kt}$$

and substitution into equation A7 yields

$$q_j(t) = \sum_j k_{ij}[A_{j1} \int_0^t (1 + \tau)e^{-\alpha 1\tau}\, d\tau + \sum_{k=2}^{3} A_{jk} \int_0^t e^{-\alpha k\tau}\, d\tau] + q_i(0) \quad \text{(Eq. A9)}$$

Equations A7, A8 and A9 lend themselves directly to a solution. In particular, this procedure requires the data to be fitted first to equation A1 or A2. Since the linear term is important only for $t < 1/\lambda_1$ (that is, 3 min), actually the experimental data were fitted to a function of type:

$$Y_j(t) \cong 2\, A_{j1}e^{-\lambda 1t} + \sum_{i=2}^{3} A_{ji}e^{-\lambda it}$$

Thus, initial estimates of the A_{jk} and α_k are required. Then, the calculated q_i (t) are fitted to the experimental data. This procedure is repeated iteratively until the values of the variable parameters are adjusted until a least square fit of the data are obtained by using an algorithm for minimizing the nonlinear function [20].

REFERENCES

1. Sapirstein LA, Vidt DG, Mandel MJ, Hanusek G: Volumes of distribution and clearances of intravenously injected creatinine in the dog. *Am J Physiol* 181:330–336, 1955
2. Blaufox MD, Orvis AL, Owen CA Jr: Compartment analysis of the radiorenogram and distribution of Hippuran I^{131} in dogs. *Am J Physiol* 204:1059–1064, 1963
3. Van Stekelenburg LHM, Al N, Truijens JHJ, Van Vals GH, Kooman A: A quantitative theory of radioisotope renography with hippuran-^{131}I. *Phys Med Biol* 11:451–460, 1966
4. Tauxe WN, Maher FT, Taylor WT: Effective renal plasma flow: Estimation from theoretical volumes of distribution of intravenously injected ^{131}I orthoiodohippurate. *Mayo Clin Proc* 46:524–531, 1971
5. Degrazia JA, Scheibe PO, Jackson PE, Lucas ZJ, Fair WR, Vogel JM, Blumin LJ: Clinical applications of a kinetic model of hippurate distribution and renal clearance. *J Nucl Med* 15:102–114, 1974
6. Van Stekelenburg LHM, Al N, Kooman A, Tertoolen JFW: A three-compartment model for the transport and distribution of hippuran. *Phys Med Biol* 21:74–84, 1976
7. Wolf IH, Buttermann G, Pabst HW: Determination of total, divided and regional tubular clearance and excretion by compartmental analysis of camera renograms. *Contr Nephrol* 11:50–54, 1978
8. Houston AS, Sampson WFD, Macleod MA: A compartmental model for the distribution of ^{113m}In-DTPA and ^{99m}Tc-(sn)DTPA in man following intravenous injection. *Int J Nucl Med Biol* 6:85–95, 1979
9. Stabin M, Taylor A Jr, Eshima D, Wooter W: Radiation dosimetry for Technetium-99m-MAG_3, Technetium-99m-DTPA, and Iodine-131-OIH based on human biodistribution studies. *J Nucl Med* 33:33–40, 1992
10. Tonnesen KH, Munck O, Hald T, Mogensen P, Wolf H: Influence on the radiorenogram of variation in skin-to-kidney distance and the clinical importance thereof, in *Radionuclides in Nephrology*, edited by Winkel SUM, Blaufox MD, Bretano JLF, Stuttgart, Georg Thieme, 1975, pp 76–86
11. Early PJ, Razzak MA, Sodee DB: *Texbook of Nuclear Medicine Technology*. St. Louis, Mosby, 1979, pp 115–118
12. Sharney L, Wasserman LR, Gevirtz NR, Schwartz L, Levitan R, Garcia AM, Leavitt D, Tendler D: Studies in iron kinetics. II. Interpretation of experimental data in terms of multiple pool systems. *J Mt Sinay Hosp* 23:305–322, 1965
13. Rutland MD: A comprehensive analysis of DTPA renal studies. *Nucl Med Commun* 6:11–30, 1985
14. Rehling M, Moller ML, Lund JO, Thamdrup B, Trap-Jensen J: Tc-99m DTPA gamma camera renography: Normal values and rapid determination of single kidney glomerular filtration rate. *Eur J Nucl Med* 11:1–6, 1985
15. Patlak CS, Blasberg RG, Fenstermacher JD: Graphical evaluation of blood to brain transfer constant from multiple time uptake data. *J Cereb Blood Flow Metab* 3:1–7, 1983
16. Jacquez JA: *Compartmental Analysis in Biology and Medicine*. Amsterdam, Elsevier Publishing Company, 1972
17. Rescigno A: *Compartmental Distribution of Radiotracers*. Edited by Robertson JS, Boca Raton, Florida, 1983
18. Wang CY: Resonance effect in compartmental analysis and its detection. *Math Biosc* 36:109–113, 1977
19. Berman M, Weiss MF: *SAAM Manual*. U.S. Department of Health, Education, and Welfare, Publication No (NIH) 78–180, Washington, D.C., 1978
20. Powell MJD: A method for minimizing a sum of squares of non linear functions without calculating derivatives. *Comp J* 7:303–307, 1965
21. Berman M, Shahn E, Weiss MF: The routine fitting of kinetics data to models: A mathematical formalism for digital computers. *Biophys J* 2:275–287, 1962
22. Berman M, Weiss MF, Shahn E: Some formal approaches to the analysis of kinetic data in terms of linear compartmental systems. *Biophys J* 2:289–316, 1962
23. Russell CD, Thorstad B, Yester MV, Stutzman M, Dubovsky EV: Quantitation of renal function with Tc-99m-MAG_3. *J Nucl Med* 29:1931–1933, 1988
24. Russell CD, Taylor A, Eshima D: Estimation of Technetium-99m-MAG_3 plasma clearance in adults from one or two blood samples. *J Nucl Med* 30:1955–1959, 1989
25. Fresco GF, Digiorgio F, Curti GL: Simultaneous estimation of glomerular filtration rate and effective renal plasma flow after a single injection of ^{51}Cr-EDTA and ^{99m}Tc-MAG_3. *J Nucl Med* 36:1701–1706, 1995
26. Blaufox MD, Merill JP: Compartmental analysis of the hippuran-^{131}I-renogram in man. *Fed Proc Fed Am Socs Exp Biol* 24:405–412, 1965
27. Jafri RA, Britton KE, Nimmon CC, Solanki K, Al-Nahhas A, Bomanji J, Fettich J, Hawkins LA: Technetium-99m MAG_3, a comparison with iodine-123 and iodine-131 orthoiodohippurate, in patients with renal disorders. *J Nucl Med* 29:147–158, 1988
28. Bubeck B, Brandau W, Weber E, Klble T, Parekh N, Georgi P: Pharmaco-kinetics of technetium-99m-MAG_3 in humans. *J Nucl Med* 31:1285–1293, 1990
29. Brochner-Mortensen J: A simple method for the determination of glomerular filtration rate. *Scand J Clin Lab Invest* 30:271–274, 1972
30. Morgan WD, Birks JL, Sivyer A, Ghose RR: An efficient technique for the simultaneous estimation of GFR and ERPF, involving a single injection and two blood samples. *Int J Nucl Med Biol* 4:79–83, 1977
31. Gordon I, Anderson PJ, Orton M, Evans K: Estimation of Technetium-99m-MAG_3 renal clearance in children: Two gamma camera techniques compared with multiple plasma samples. *J Nucl Med* 32:1704–1708, 1991
32. Bubeck B: Renal clearance determination with one blood sample: Improved accuracy and universal applicability by a new calculation principle. *Semin Nucl Med* 23:73–86, 1993
33. Nielsen SP, Moller ML, Trap-Jensen J: ^{99m}Tc-DTPA scintillation camera renography: A new method for estimation of single-kidney function. *J Nucl Med* 18:112–117, 1977
34. Assailly J, Pavel DG, Bader C, Chanard J, Ryerson TW, Cotard JP, Funck-Brentano JL: Noninvasive experimental determination of the individual kidney filtration fraction by means of a dual-tracer technique. *J Nucl Med* 18:684–691, 1977
35. Schlegel JU, Hamway SA: Individual renal plasma flow determination in 2 minutes. *J Urol* 116:282–285, 1976
36. Gates GF: Glomerular filtration rate: Estimation from fractional renal accumulation of ^{99m}Tc-DTPA (stannous). *Am J Radiol* 138:565–570, 1982
37. Lee TY, Constable AR, Cranage RW: A method for GFR determination without blood samples in routine renal scintigraphy with Tc-99m-DTPA, in *Radionuclides in Nephrology*, edited by Joekes AM, Constable AR, Brown NJG, Tauxe WN, London, Academic Press, 1982, pp 107–112